NASA Technical Memorandum

NASA TM-100374

THE EFFECTS OF TEMPERATURE GRADIENT AND GROWTH RATE ON THE MORPHOLOGY AND FATIGUE PROPERTIES OF MAR-M246(Hf)

Center Director's Discretionary Fund Final Report

By D. D. Schmidt, W. S. Alter, W. D. Hamilton, and R. A. Parr

Materials and Processes Laboratory
Science and Engineering Directorate

August 1989

National Aeronautics and Space Administration

George C. Marshall Space Flight Center

TECHNICAL REPORT STANDARD TITLE PAGE

1. REPORT NO.	2. GOVERNMENT ACCESSION NO.	3. RECIPIENT'S CATALOG NO.
NASA TM -100374		

4. TITLE AND SUBTITLE	5. REPORT DATE
The Effects of Temperature Gradient and Growth Rate on the Morphology and Fatigue Properties of MAR-M246(Hf) Center Director's Discretionary Fund Final Report	August 1989
	6. PERFORMING ORGANIZATION CODE
7. AUTHOR(S) D. D. Schmidt, W. S. Alter, W. D. Hamilton, and R. A. Parr	8. PERFORMING ORGANIZATION REPORT #
9. PERFORMING ORGANIZATION NAME AND ADDRESS George C. Marshall Space Flight Center Marshall Space Flight Center, Alabama 35812	10. WORK UNIT NO.
	11. CONTRACT OR GRANT NO.
	13. TYPE OF REPORT & PERIOD COVERED Technical Memorandum
12. SPONSORING AGENCY NAME AND ADDRESS National Aeronautics and Space Administration Washington, D.C. 20546	14. SPONSORING AGENCY CODE

15. SUPPLEMENTARY NOTES
Prepared by Materials and Processes Laboratory, Science and Engineering Directorate.

16. ABSTRACT

MAR-M246(Hf) is a nickel-based superalloy used in the turbopump blades of the Space Shuttle main engines. This study considers the effect of temperature gradient (G) and growth rate (R) on the microstructure and fatigue properties of this superalloy. The primary dendrite arm spacings were found to be inversely proportional to both temperature gradient and growth rate. Carbide and γ-γ' morphology trends were related to G/R ratios. Weibull analysis of fatigue results shows the characteristic life to be larger by a factor of 10 for the low gradient/fast rate pairing of G and R, while the reliability (β) was lower.

17. KEY WORDS	18. DISTRIBUTION STATEMENT
Superalloy, temperature gradient (G), growth rate (R), G/R ratios, fatigue properties, carbide morphology	Unclassified – Unlimited

19. SECURITY CLASSIF. (of this report)	20. SECURITY CLASSIF. (of this page)	21. NO. OF PAGES	22. PRICE
Unclassified	Unclassified	24	NTIS

MSFC - Form 3292 (May 1969)

For sale by National Technical Information Service, Springfield, Virginia 22151

TABLE OF CONTENTS

LIST OF ILLUSTRATIONS

TECHNICAL MEMORANDUM

THE EFFECTS OF TEMPERATURE GRADIENT AND GROWTH RATE ON THE FATIGUE PROPERTIES AND MORPHOLOGY OF MAR-M246(Hf)

INTRODUCTION

MAR-M246(Hf) is a nickel-based superalloy used in the turbopump blades of the Space Shuttle Main Engines. Enhancement of the fatigue properties of this alloy would extend the life span of these blades, thus reducing the cost per flight. Enhancement has been attempted by studying the heat treatment and growth rate [1,3,6]. This study considers the effects of temperature gradient and growth rate on the microstructure and the fatigue properties of this superalloy.

Present processing parameters of the turbine blades do not take into consideration how carbide morphology affects the resistance to fatigue cracking, or the role that the γ-γ' eutectic plays. The debate continues as to which carbide morphology, block or script type, promotes crack initiation and propagation. The correct pairing of temperature gradient (G) and growth rate (R) needed to produce a specific morphology are also not universally agreed upon.

Control of the dendrite arm spacings must be considered as a possible enhancement to the fatigue properties of this superalloy. The complicating factor, as previous studies have indicated, is that the faster solidification rates predicted to produce the preferred dendritic arm spacing [2,3] are also predicted to produce the coarse script carbide when processed at temperature gradients commonly used in commercial directional solidification growth conditions [4]. These script carbides have been argued to be more instrumental in the cracking problems of this nickel-based alloy [5].

However, the literature presents conflicting results on predicting a carbide morphology based on a temperature gradient and a solidification rate. Studies have been conducted which imply that high G/R ratios are needed to produce carbides with a block appearance, while low G/R ratios produce script type [7,8], i.e., should G be held constant and R increased, then the script morphology should predominate. Yet in another study, it was stated that, "These carbides exhibit an equiaxed faceted particle morphology in rapidly-cooled regions, and a script morphology in slowly-cooled regions in directionally solidified dendritic alloys" [9].

PROCEDURE

Three different temperature gradients were selected to directionally solidify (DS) MAR-M246(Hf) at two different translation rates. The temperature gradients were achieved via a furnace with three cores, each controlled independently. The gradients selected were 68 °C/cm, 170 °C/cm, and 309 °C/cm with solidification rates of 5 cm/hr and 30 cm/hr. The specimens were then heat treated using the standard treatment [1] and the resulting microstructure metallographically examined.

MECHANICAL TESTING

The fatigue specimens were tested for high cycle fatigue (HCF) at room temperature in air with a minimum/maximum ratio (R) of 0.4, and a maximum stress level of 125 ksi. These maximum stress levels were selected from a pre-determined expected life. Fatigue test data were then analyzed using the Weibull technique.

The Weibull technique is a statistical method of analyzing failures and predicting life expectancy. The approach is based on the equation:

$$F(t) = 1 - e^{-[(t-t_o)/\eta]^{\beta}}$$

where

$F(t)$ = fraction failing

t = time to failure

t_o = starting time

η = characteristic life

β = slope .

A ranked regression and plotting on Weibull paper allows the determination of the characteristic life for all samples tested under similar conditions. The slope of the best fitting line (β) predicts the type of failures to be expected:

0 - 1 infant mortality

1 - 3 early wear out

4 - 6 normal wear out [10].

RESULTS

A matrix of temperature gradient and solidification rates has been prepared and is presented in Table 1 in ascending order of G/R ratios; also included are primary dendrite arm spacings (λ) and time (t) spent in the mushy zone of the furnace. The mushy zone is that portion of the directional solidification furnace that lies between the liquidus and solidus temperatures of the superalloy. The primary dendrite arm spacing measurements in Table 1 are indirectly proportional to the growth rate and the temperature gradient. Typical microstructures representing the temperature gradients and solidification rates are presented in Figures 1 through 6. Figures 1 through 3 show that the primary dendrite arm spacings from the 30 cm/hr rate are smaller than that of the 5 cm/hr rate, and decrease with increasing G.

Figures 4 through 6 show that at the fast solidification rate, the small fine block carbides exhibit a shift to a small fine, more script-type morphology as the temperature gradient increases. This shift is quite evident between the intermediate gradient of 170 °C/cm and the high gradient of 309 °C/cm. The 170 °C/cm gradient has the small fine block morphology seen in the 68 °C/cm gradient with slight indications of script transition beginning. The 309 °C/cm gradient clearly shows that a small fine script morphology has developed. Large, irregular block carbides can be seen in almost equal quantities to the large and extremely coarse script-type carbides formed at the high gradient of 309 °C/cm and slow rate of 5 cm/hr (Fig. 6B) with the intermediate gradient of 170 °C/cm and the same slow rate producing small coarse script-type carbides (Fig. 5B). The low gradient and slow rate specimens contain a large fine script carbide morphology (Fig. 4B).

Figures 4 through 6 clearly indicate that large γ-γ' eutectic islands are formed at the slow solidification rate. The fast rate/high gradient had smaller clumps of eutectic phase than is seen in the slower growth rate specimens. No eutectic phase is detectable in the low 68 °C/cm gradient and fast rate.

CONCLUSION

At a fast solidification rate, the carbide morphology seems to be changing from a small fine block to a small fine script as temperature gradient is increased. A coarsening trend appears in the slow rate as the temperature gradient increases, along with the appearance of large irregular block carbides. There appears to be a correlation between carbide type and G/R ratio. For low ratios (less than 10), the morphology is block with script appearing at G/R = 10.3. As G/R increases from 10.3, the script carbides appear to coarsen and irregular blocks become more prominent. However, it should be pointed out that two completely different sets of conditions could yield the same G/R ratios. For example, a G/R = 10.3 can be achieved with a high G = 309 °C/cm and fast R = 30 cm/hr, or a low G = 51.5 °C/cm and a slow R = 5 cm/hr. For this study, both sets of conditions did produce a fine script. The low gradient/slow rates' larger script size may be attributed to more time spent in the mushy zone. However, results from this study indicate that G/R ratios alone may be insufficient to predict carbide behavior. Specifically, this study shows that low G/R ratios of 2.2 and 5.7 produce a small block whereas there are results presented in the literature [7,8] that show a high ratio produces block. With these conflicts in mind, perhaps G and R have a more complex relationship to carbide morphology than a simple ratio. In fact, the actual temperature profile may be a significant contributing factor to the resulting microstructure. This possibility is currently under investigation with a respective paper planned for submission at a later date.

A large block carbide that was suspected not to have melted during processing but instead coarsened was associated with crack formation for the alloy MAR-M200 [11]. Another study of MAR-M246(Hf) suggests that face crack origins are exclusively associated with carbide structure [12]. The carbide phase depicted appears to be a script-type. Perhaps these suspect crack-causing carbides are the same type, but because the orientational relationships of the carbides to the matrix may be different, the carbides may appear as having different morphologies. A study has been conducted which metallographically examined the (011), the (112), and the (111) planes of a DS MAR-M200 sample. "Inspection of the (001) section reveals that the ...carbide appears as needles aligned parallel to the <011> directions." "Consideration of these three sections indicates that the ..carbide actually has a platelet morphology lying

parallel to the {111} planes of the matrix" [13]. Figure 13 shows the interconnecting platelets of a script carbide. The matrix was partially electrochemically etched away to reveal the carbide morphology in detail. Thus, morphology may at times be incorrectly categorized. This possibility could bear some thought when fracture origins are examined and a carbide is found to be the initiator.

Table 2 presents high cycle fatigue (HCF) data for two temperature gradients (G) and growth rates (R). Weibull analysis was performed in all cases and showed that G = 170 °C/cm and the slow rate of 5 cm/hr produced a larger (β) which signifies a more predictable fatigue life. (All the Weibull analyses are represented in Figures 7 and 8). However, as in a previous study [6], the small block carbide morphology produced a larger characteristic life (η). The microstructure containing the small block morphology obtained in this study by processing at a lower G = 68 °C/cm and the same fast rate of 30 cm/hr (Fig. 4a) again has the largest characteristic life. This time η was greater by a significant factor of 5 to 10, which included fatigue data of pairings from the previous study [6]. Hence, this microstructure is considered preferable to the other microstructures tested, based on HCF test data. The predominant failure mechanism was identified as Stage 1 crystallographic high cycle fatigue; some fracture surfaces indicated failure by grain boundary cracking, ductile overload, and surface and subsurface anomalies (Fig. 11). It is suspected that design flaws in the furnace allowed oxidation during processing, which caused inclusions. Specimens with inclusions exhibited a shortened fatigue life when compared to specimens from the same pairing of G and R that did not indicate evidence of inclusions. This is exemplified by the "dog-legs" seen in Figures 7(a). A dog-leg curve generated from a Weibull analysis implies there may be different failure mechanisms involved. The four points in Figure 7(a) indicating shorter fatigue lives represent the bottom of the dog leg and specimens with inclusions. Figure 8 is the corrected Weibull analysis for G = 68 °C/cm and R = 30 cm/hr. Specimens with inclusions, and those that failed in the threads, have been placed in suspension. The characteristic life has increased to 3 million, with β also increasing to 2.88. Auger Electron Spectroscopy (AES) analysis indicated that the inclusions were aluminum oxide; processing in a vacuum should eliminate these oxides. Figure 9 represents the data points for the set: G = 68 °C/cm and R = 30 cm/hr. While all pairing contained specimens with inclusions, the preferred microstructure specimens with the shortest fatigue lives still had longer fatigue lives than almost all specimens from any of the other pairings tested.

The extension of fatigue life for the preferred microstructure may be attributed to the small, well dispersed blocky carbide; some of which appear to have adapted an almost spherical shape. The absence of visually detectable γ-γ' eutectic and small dendrite arm spacings may also have contributed to extended fatigue life results. Photomicrographs taken with a Transmission Electron Microscope (TEM) show that γ-γ' eutectic is not visible at high magnification (Fig. 12).

It is interesting to note that the next most desirable microstructure also was characterized by small, well dispersed blocky carbides and small dendrite arm spacings (DAS); however, unlike the preferred microstructure, this second choice contained a eutectic phase. As indicated in Table 2, this second choice microstructure had a characteristic life only twice that of the microstructures containing script carbide morphology, larger DAS, and eutectic. This reenforces the suggestion that the eutectic phase was influential in the HCF performance.

Results indicate that significant improvements in fatigue properties can be derived through manipulation of DS parameters. At the present time, it is recommended

that a small, well dispersed blocky carbide with small DAS microstructure, preferably without eutectic phase, be implemented throughout the current MAR-M246(Hf) SSME turbopump blades. This recommendation is based on the few pairings represented in this and another study [6]. With numerous combinations left unexplored, there is potential for further improvement.

Extensive further study is planned using a more advanced system and an extremely controlled environment for DS processing than was previously available. A large number of gradients and rates will be processed and tested for improved fatigue properties, as well as a more precise G and R relationship to carbide behavior. Upon completion of this extended study, a final definition of DS processing parameters will be recommended for turbine blade casting procedures.

REFERENCES

1. McCay, M.H., Schmidt, D.D., Alter, W.S., Hamilton, W.D., and Parr, R.A.: Heat Treatment Study of MAR-M246(Hf). NASA Technical Memorandum (to be published), 1987.

2. Tien, J.K., and Gamble, R.P.: The Suppression of Dendritic Growth in Nickel-Base Superalloys During Unidirectional Solidification. Mater. Sci. Eng., Vol. 8, 1971, p. 155, 159.

3. Johnston, M.H., and Parr, R.A.: A Study of the Solidification Parameters Influencing Structure and Properties in MAR-M246(Hf). NASA Technical Memorandum-82569, 1984.

4. NASA SSME Turbine Blade Analysis Team Report No. RSS-8732, p. 8-10.

5. NASA SSME Turbine Blade Analysis Team Report No. RSS-8732, p. 8-8.

6. McCay, M.H., Schmidt, D.D., Hamilton, W.D., Alter, W.S., and Parr, R.A.: The Influence of Growth Rate on the Fatigue Properties in a Directionally Solidified Superalloy. NASA Technical Memorandum (to be published), 1987.

7. McLean, M.: Directionally Solidified Materials for High Temperature Service. The Metals Society 1983, London, England, p. 43.

8. Fernandez, R., Lacomte, J.C., and Kattamis, T.Z.: Effect of Solidification Parameters on the Growth Geometry of MC Carbide in IN-100 Dendritic Monocrystals. Metallurgical Transactions A, Vol. 9A, 1978, p. 1384.

9. Sellamuthu, R., and Giamei, A.F.: Measurement of Segregation and Distribution Coefficients in MAR-M200 and Hafnium-Modified MAR-M200 Superalloys. Metallurgical Transactions A, Vol. 17A, 1986, p. 419.

10. Abernethy, R.B., Breneman, J.E., Medlin, C.H., and Reinman, G.L.: Weibull Analysis Handbook. Final Report, AFWAL-TR-83-2079, November 1983.

11. Fernandez, R., Lacomte, J.C., and Kattamis, T.Z.: Effect of Solidification Parameters on the Growth Geometry of MC Carbide in IN-100 Dendritic Monocrystals. Metallurgical Transactions A, Vol. 9A, 1978, p. 1383.

12. NASA SSME Turbine Blade Analysis Team Report No. RSS-8732, p. 5-32.

13. Piearcey, B.J., and Smashey, R.W.: The Carbide Phases in MAR-M200. Transactions of the AIME, Vol. 239, 1967.

TABLE 1

Low Gradient Fast Rate	Inter. Gradient Fast Rate	High Gradient Fast Rate	Low Gradient Slow Rate	Inter. Gradient Slow Rate	High Gradient Slow Rate
G = 68 °C/cm R = 30 cm/hr G/R = 2.2 λ = .16 mm t = 5 min	G = 170 °C/cm R = 30 cm/hr G/R = 5.7 λ = .15 mm t = 2 min	G = 309 °C/cm R = 30 cm/hr G/R = 10.3 λ = .11 mm t = 1.1 min	G = 68 °C/cm R = 5 cm/hr G/R = 13.6 λ = .37 mm t = 30 min	G = 170 °C/cm R = 5 cm/hr G/R = 34 λ = .26 mm t = 12 min	G = 309 °C/cm R = 5 cm/hr G/R = 61.8 λ = .17 mm t = 6.6 min
Small discrete blocky carbides	Small discrete blocky carbides	Small fine script carbides	Large fine script carbides	Small course script carbides	Large course script/large irregular block carbides
virtually no eutectic	small eutectic clumps	small eutectic clumps	large eutectic islands	large eutectic islands	large eutectic islands

TABLE 2

Large Fine Script Large Eutectic Islands	Small Course Script Large Eutectic Islands	Small Block Virtually No Eutectic	Small Block Small Eutectic Clumps
G = 68 °C/cm R = 5 cm/hr β = 1.38 η = 0.14M*	G = 170 °C/cm R = 5 cm/hr β = 3.09 η = 0.12M*	G = 68 °C/cm R = 30 cm/hr β = 1.2 η = 1.26M*	G = 170 °C/cm R = 30 cm/hr β = 0.83 η = 0.23M*

* M = million cycles

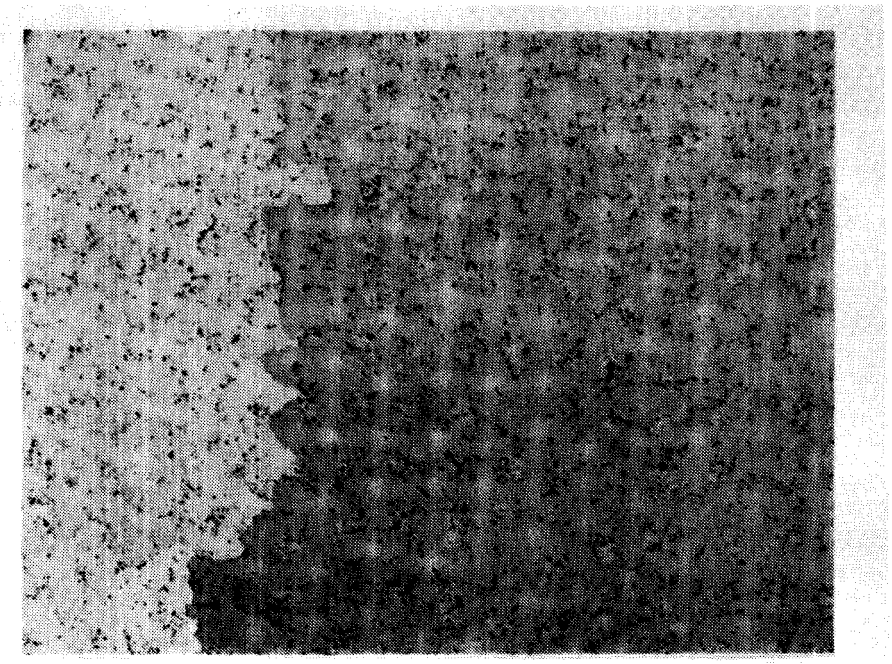

A. G=68°C/cm R=30cm/hr 50X

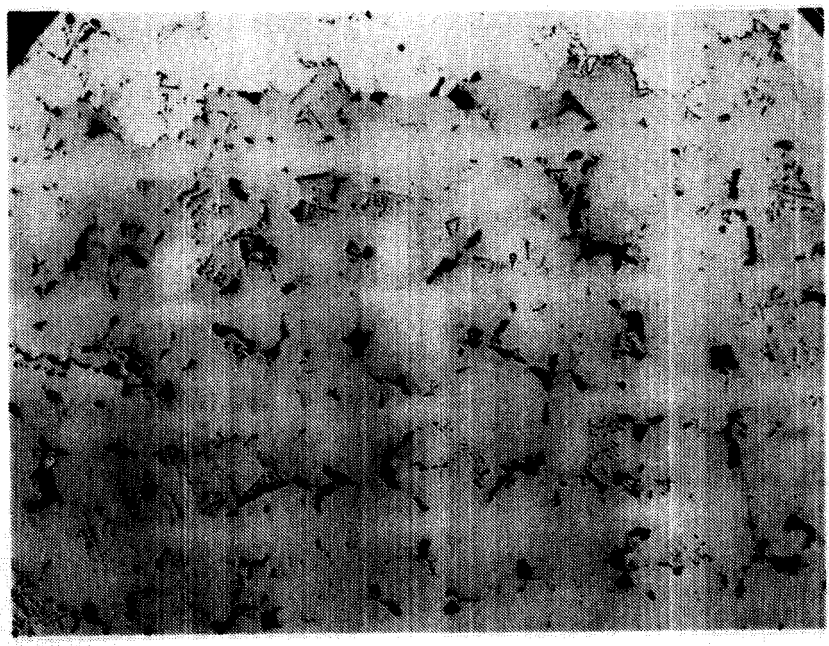

B. G=68°C/cm R=5cm/hr 50X

Figure 1. Primary dendrite arm spacings at G = 68 °C/cm and two different growth rates.

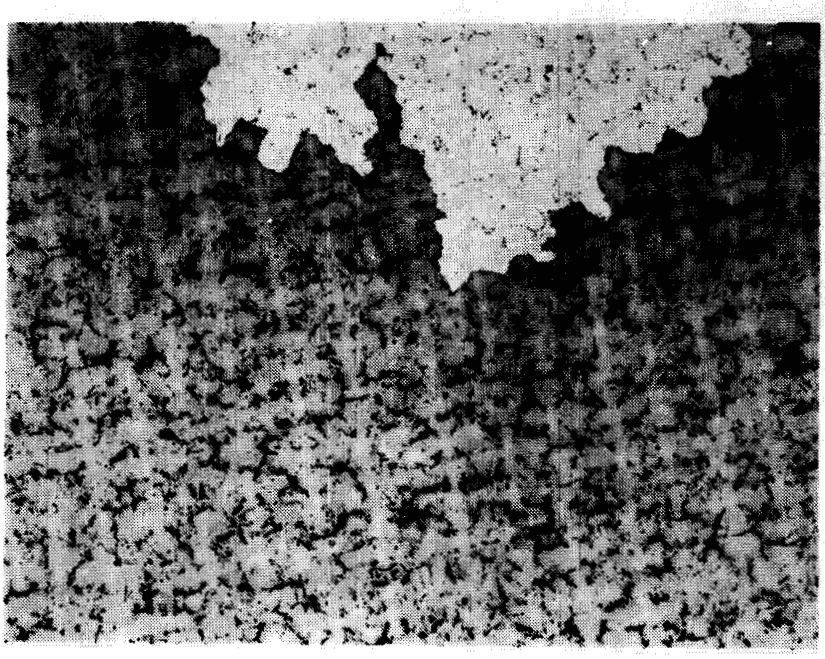

A. G=170°C/cm R=30cm/hr 50X

B. G=170°C/cm R=5cm/hr 50X

Figure 2. Primary dendrite arm spacings at G = 170 °C/cm and two different growth rates.

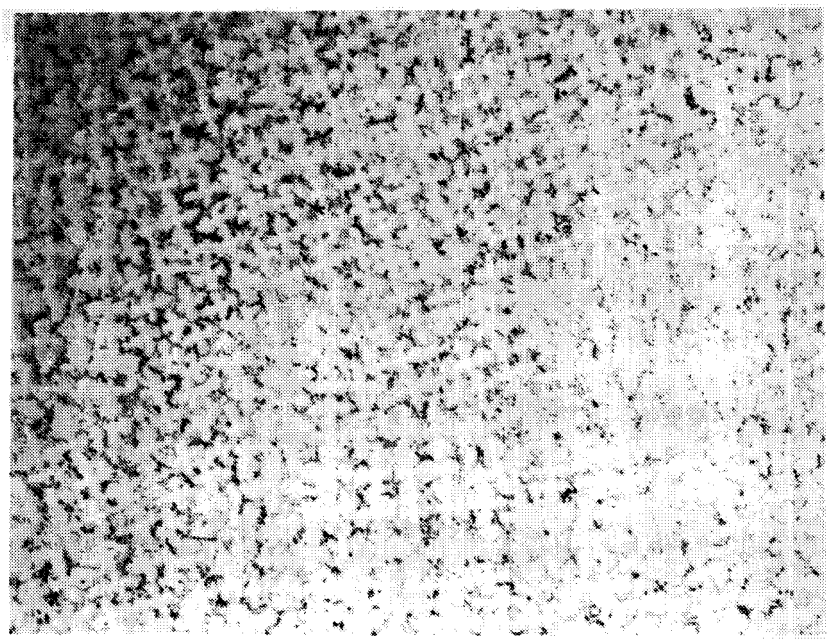

A. G=309°C/cm R=30cm/hr 50X

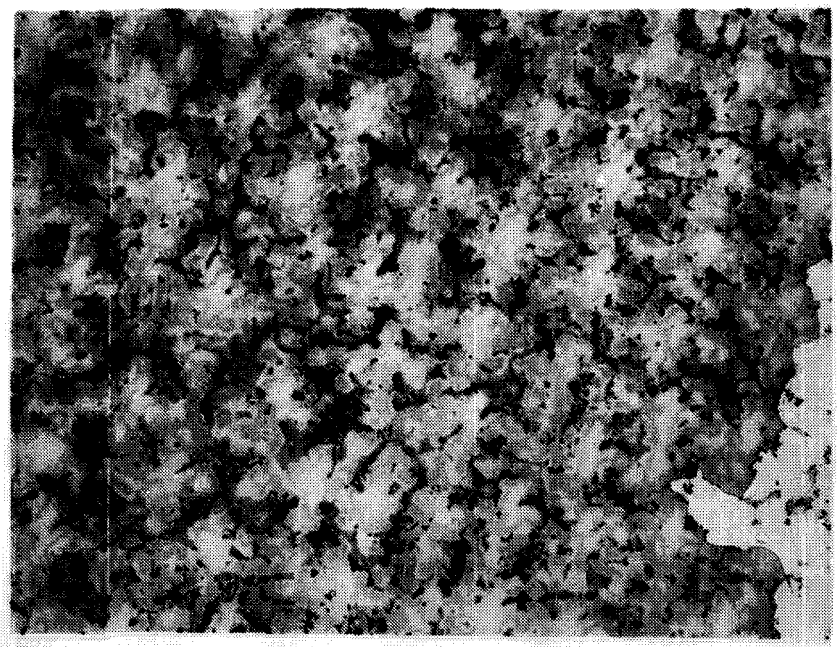

B. G=309°C/cm R=5cm/hr 50X

Figure 3. Primary dendrite arm spacing at G = 309 °C/cm and two different growth rates.

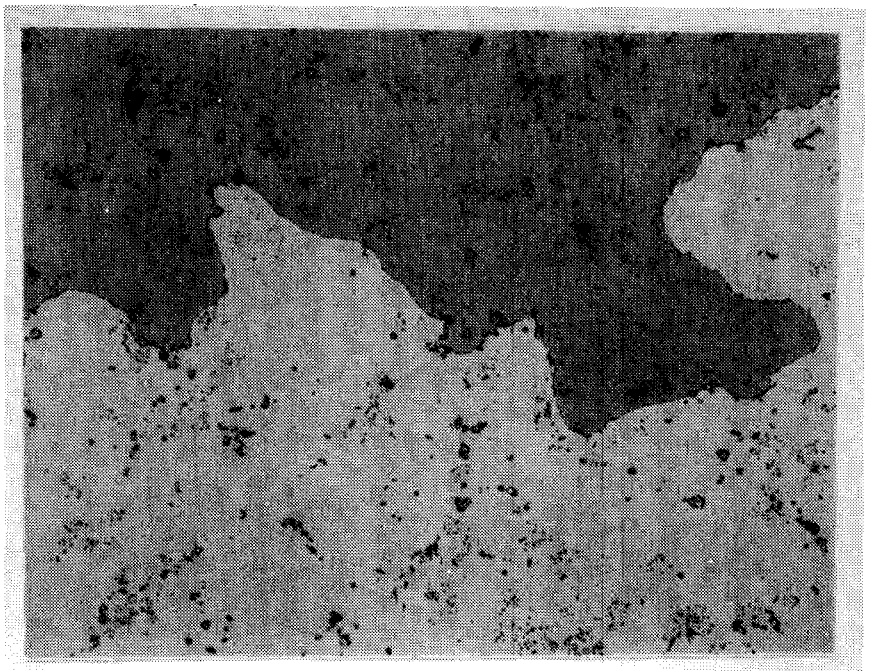

A. G=68°C/cm R=30cm/hr 200X

B. G=68°C/cm R=5cm/hr 200X

Figure 4. Carbide and γ-γ' eutectic morphology at G = 68 °C/cm and two different growth rates.

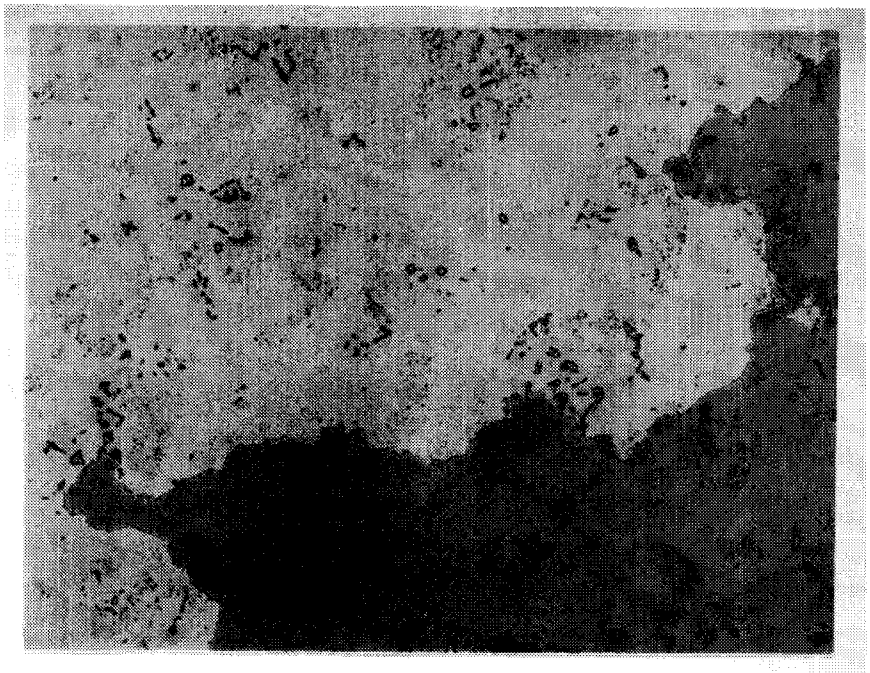

A. G=170°C/cm R=30cm/hr 200X

B. G=170°C/cm R=5cm/hr 200X

Figure 5. Carbide and γ-γ' eutectic morphology at G = 170 °C/cm and two different growth rates.

A. G=309 °C/cm R=30 cm/hr 200X

B. G=309 °C/cm R=5 cm/hr 200X

Figure 6. Carbide and γ-γ' eutectic morphology at G = 309 °C/cm and two different growth rates.

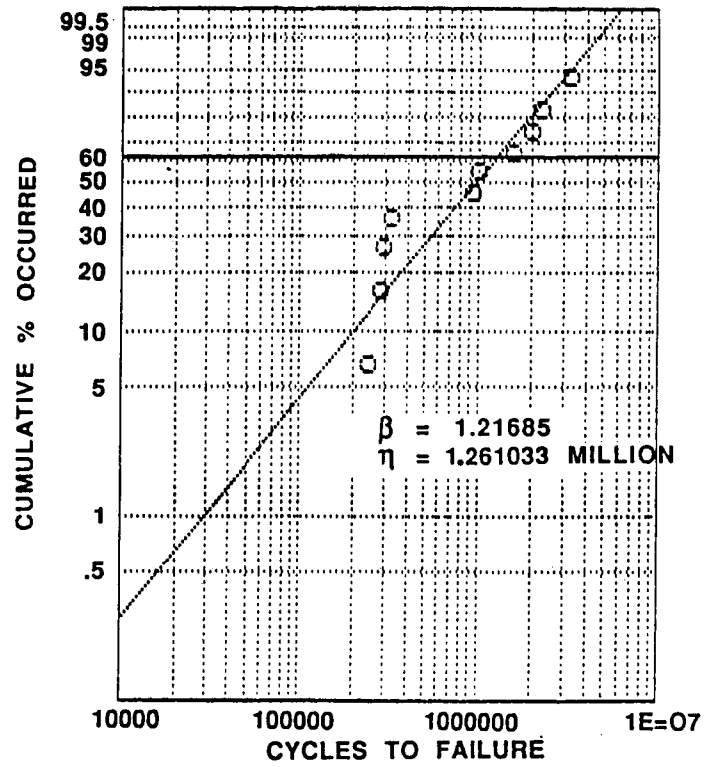

Figure 7(a). Weibull analysis plots for G = 68 °C/cm and R = 30 cm/hr.

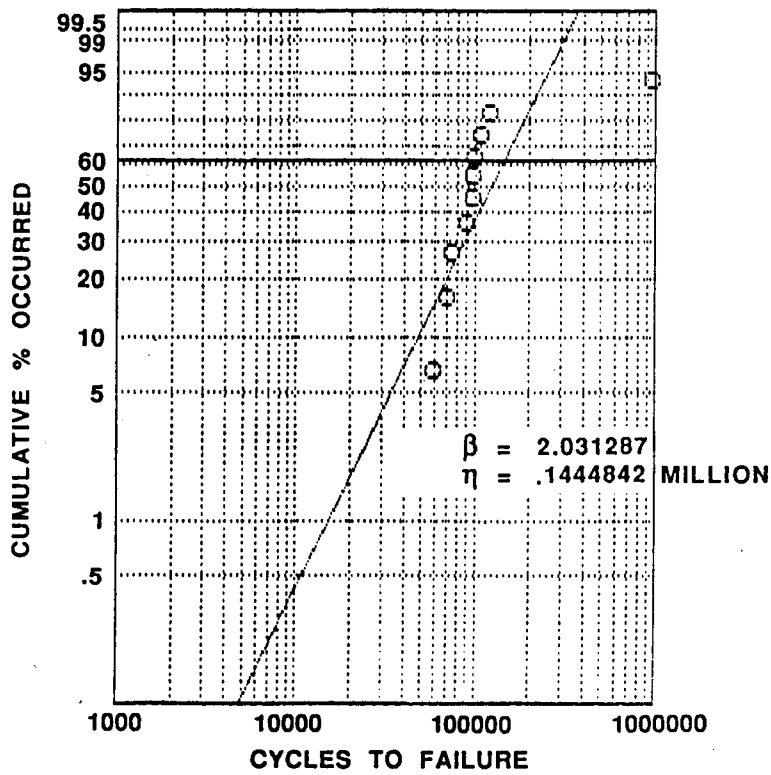

Figure 7(b). Weibull analysis plots for G = 68 °C/cm and R = 5 cm/hr.

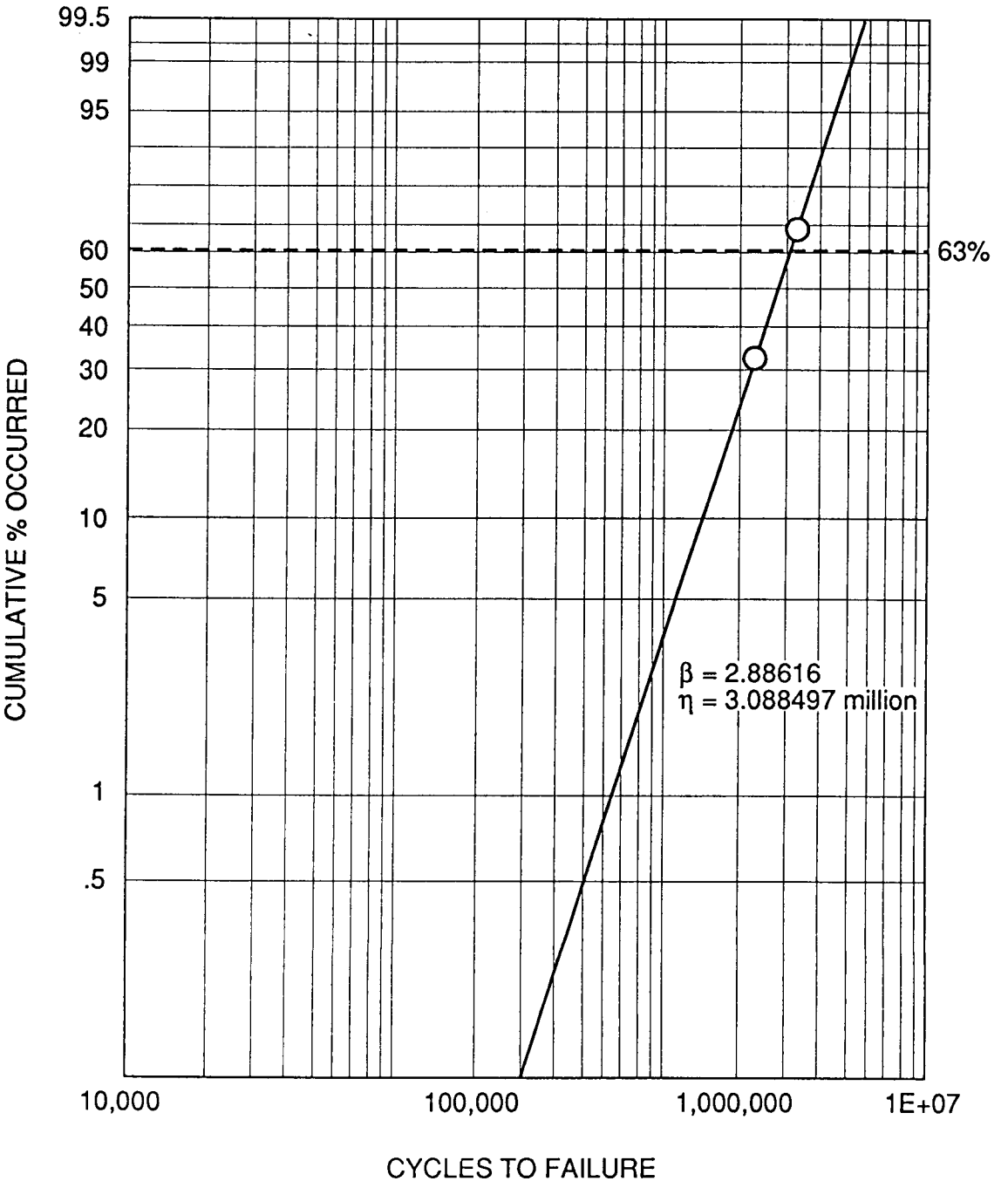

Figure 8. Corrected Weibull analysis plot of fatigue data for G = 68 °C/cm and R = 30 cm/hr.

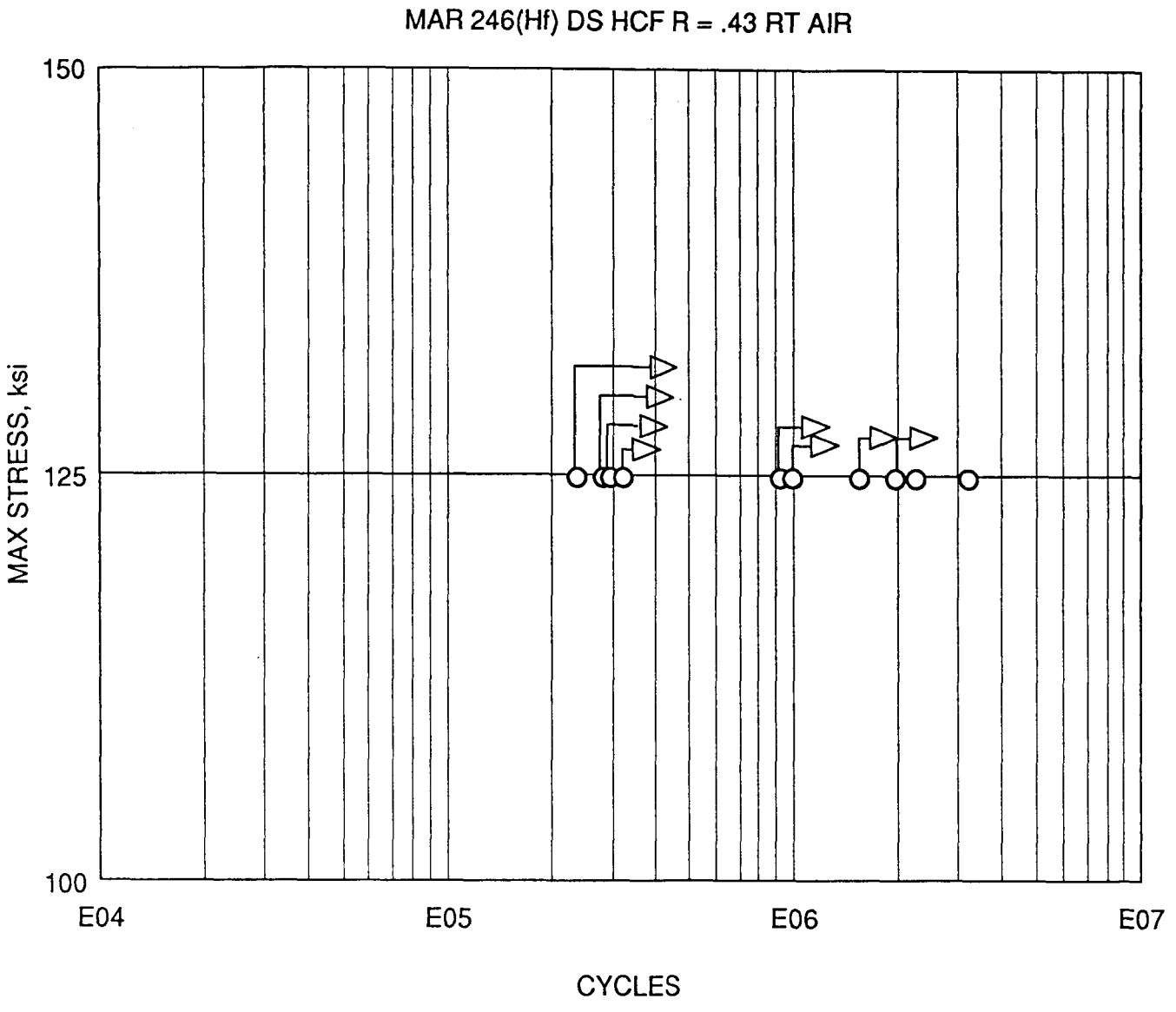

Figure 9. Data points for G = 68 °C/cm and R = 30 cm/hr.

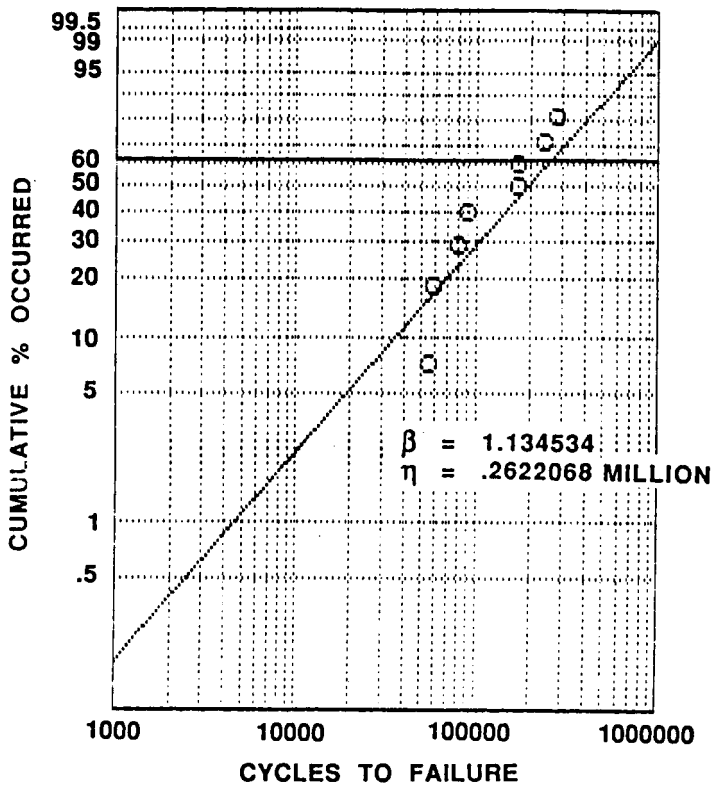

Figure 10(a). Weibull analysis plots for G = 170 °C/cm and

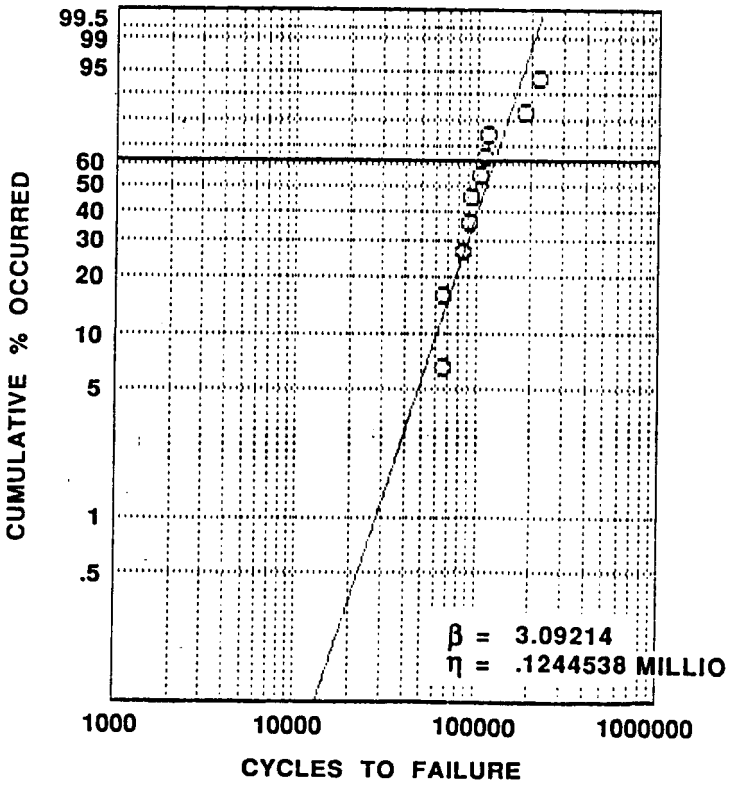

Figure 10(b). Weibull analysis plots for G = 170 °C/cm and

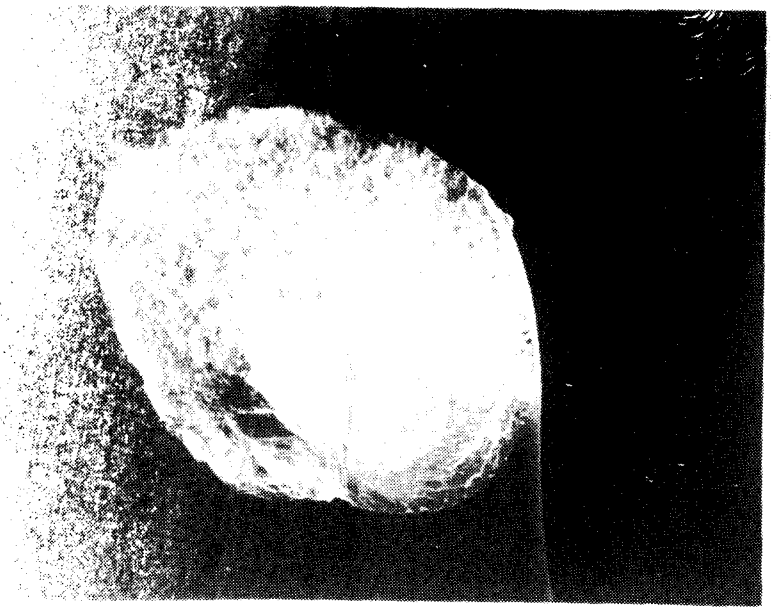

25X

(a). High cycle fatigue specimen after fracture.

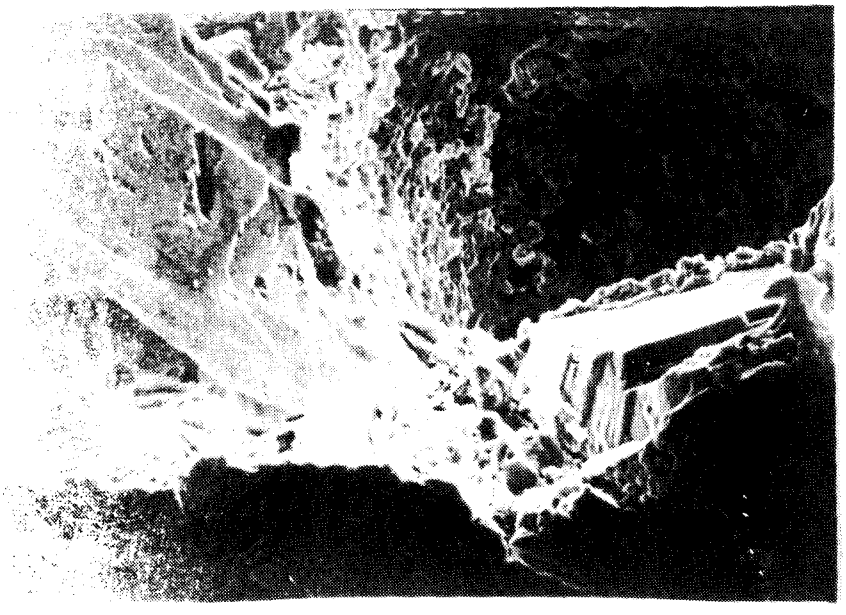

1000X

(b). Fracture site showing oxidative inclusions.

Figure 11. Scanning Electron Microscope photomicrographs of a fra
specimen directionally solidified at G = 68 °C/cm and R = 30 cm

Figure 12. Transmission Electron Microscope (TEM) photomicrograph of the γ' phase for G = 68 °C/cm and R = 30 cm/hr.

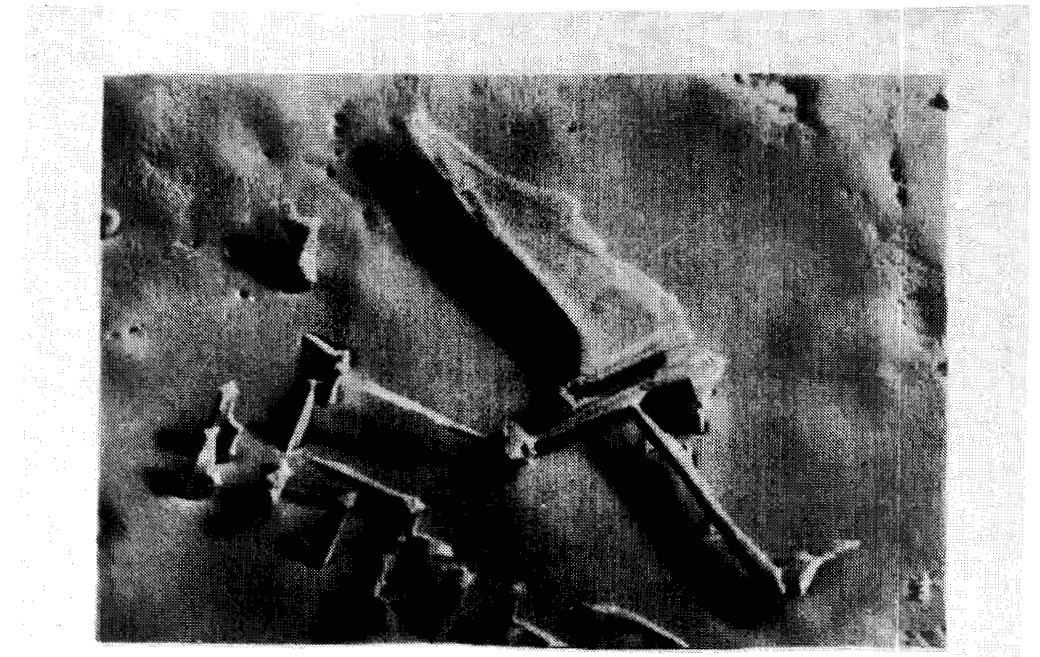

1000x

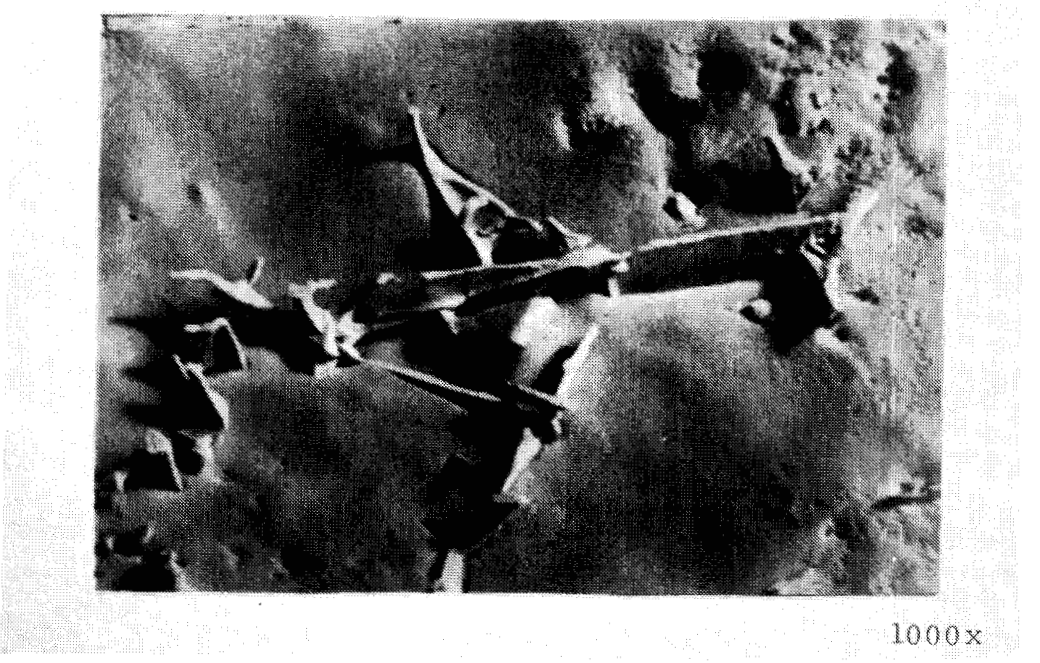

1000x

Figure 13. Scanning Electron Microscope (SEM) photomicrographs of MAR-M246(Hf) electrochemically etched to reveal the interconnecting platelets of a script carbide.

APPROVAL

THE EFFECTS OF TEMPERATURE GRADIENT AND GROWTH RATE ON THE MORPHOLOGY AND FATIGUE PROPERTIES OF MAR-M246(Hf)

Center Director's Discretionary Fund Final Report

By D. D. Schmidt, W. S. Alter, W. D. Hamilton, and R. A. Parr

The information in this report has been reviewed for technical content. Review of any information concerning Department of Defense or nuclear energy activities or programs has been made by the MSFC Security Classification Officer. This report, in its entirety, has been determined to be unclassified.

C. F. Key

P. H. SCHUEREN
Director, Materials and Processes Laboratory

☆U.S. GOVERNMENT PRINTING OFFICE 1989: - 631-056/00170